Published in final edited form as:
Environ Sci Technol. 2022 April 05; 56(7): 3894–3904. doi:10.1021/acs.est.1c05634.

Global Emissions of Hydrogen Chloride and Particulate Chloride from Continental Sources

Bingqing Zhang[1], **Huizhong Shen**[2], **Xiao Yun**[3], **Qirui Zhong**[4], **Barron H. Henderson**[5], **Xuan Wang**[6], **Liuhua Shi**[7], **Sachin S. Gunthe**[8,9], **Lewis Gregory Huey**[1], **Shu Tao**[2,3], **Armistead G. Russell**[10], **Pengfei Liu**[*,1]

[(1)]School of Earth and Atmospheric Sciences, Georgia Institute of Technology, Atlanta, Georgia 30332, USA

[(2)]School of Environmental science and Engineering, Southern University of Science and Technology, Shenzhen, Guangdong 518055, China

[(3)]College of Urban and Environmental Sciences, Laboratory for Earth Surface Processes, Sino-French Institute for Earth System Science, Peking University, Beijing 100871, China

[(4)]Department of Earth Science, Vrije Universiteit Amsterdam, 1081 HV Amsterdam, the Netherlands

[(5)]United States Environmental Protection Agency, Research Triangle Park, Durham, North Carolina 27709, USA

[(6)]School of Energy and Environment, City University of Hong Kong, Hong Kong SAR, China

[(7)]Gangarosa Department of Environmental Health, Rollins School of Public Health, Emory University, Atlanta, Georgia 30322, USA

[(8)]EWRE Division, Department of Civil Engineering, Indian Institute of Technology Madras, Chennai, Tamil Nadu 600036, India

[(9)]Laboratory for Atmospheric and Climate Sciences, Indian Institute of Technology Madras, Chennai, Tamil Nadu 600036, India

[(10)]School of Civil and Environmental Engineering, Georgia Institute of Technology, Atlanta, Georgia 30332, USA

Abstract

[*]To Whom Correspondence Should be Addressed pengfei.liu@eas.gatech.edu.

Support Information

Text S1, activity data of open waste burning estimation; Text S2, emission factor estimation; Text S3, emission driving factors decomposition; Text S4, Uncertainty analysis and comparison with other studies; Table S1, Chlorine content of produced coal in major countries; Table S2, Chlorine content of consumed coal in 222 countries; Table S3 HCl and pCl removal efficiency by pollution control devices; Table S4, Parameters of S-shaped curve for installation rate of FGD and wFGD; Table S5, emission factors of HCl for different types of waste; Table S6, Comparison of data in this study with data reported in other studies; Figure S1, Source profiles of top three HCl, pCl, and total Cl emission countries; Figure S2, Geographical distributions of HCl and pCl emissions by sectors; Figure S3, Temporal trends of regional HCl, pCl, and tCl emissions in different sectors; Temporal trends of sectorial HCl, pCl, and tCl emissions in different regions; Figure S5, Decomposition of the changes in global HCl and pCl emissions within 5 time periods.

Gaseous and particulate chlorine species play an important role in modulating tropospheric oxidation capacity, aerosol water uptake, visibility degradation, and human health. The lack of recent global continental chlorine emissions has hindered modeling studies of the role of chlorine in the atmosphere. Here we develop a comprehensive global emission inventory of gaseous HCl and particulate Cl^- (pCl), including 35 sources categorized in 6 source sectors based on published up-to-date activity data and emission factors. These emissions are gridded at 0.1° × 0.1° spatial resolution for the years 1960 to 2014. The estimated emissions of HCl and pCl in 2014 are 2354 (1661 – 3201) and 2321 (930 – 3264) Gg Cl a^{-1}, respectively. Emissions of HCl are mostly from open waste burning (38%), open biomass burning (19%), energy (19%) and residential (13%) sectors, and the major sources classified by fuel type are combustion of waste (43%), biomass (32%), and coal (25%). Emissions of pCl are mostly from biofuel (29%) and open biomass burning processes (44%). The sectoral and spatial distributions of HCl and pCl emissions are very heterogeneous along the study period, and the temporal trends are mainly driven by the changes in emission factors, energy intensity, economy, and population.

Graphical Abstract

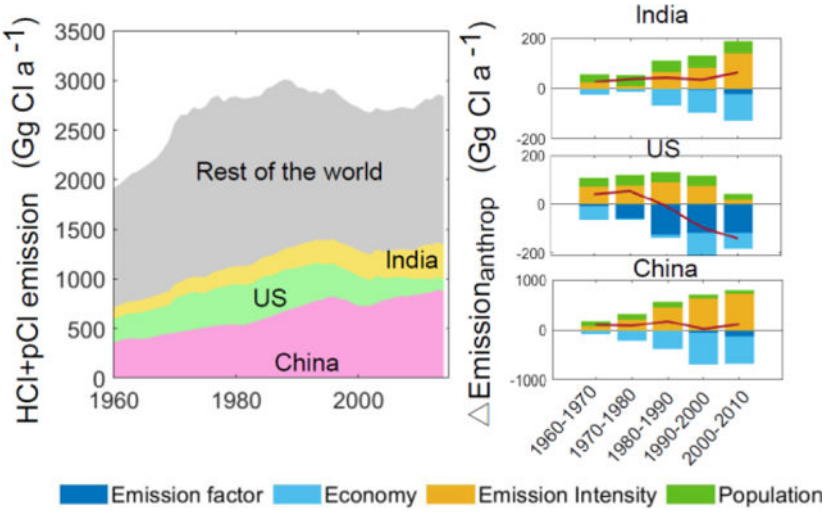

Keywords

air pollution; emission inventory; chloride; atmospheric aerosols; tropospheric chemistry

1. Introduction

Gaseous and particulate chlorine species in the troposphere can impact air quality and atmospheric chemistry. For example, gaseous hydrogen chloride (HCl) and particulate chloride (pCl) undergo gas-particle partitioning processes, affecting aerosol water uptake and enhancing fog and haze formation.[1] Particulate chloride reacts with N_2O_5 to form $ClNO_2$. The subsequent photolysis of $ClNO_2$ in the daytime releases the chlorine radical (Cl·), which can oxidize volatile organic compounds (VOCs) to further influence the formation of ozone and secondary organic aerosol (SOA).[2–4] The cycling of Cl·, other halogens, and their reservoirs can catalyze ozone depletion and oxides of nitrogen (NO_x

= NO + NO_2) conversion into nitric acid (HNO_3), thus having a profound effect on tropospheric oxidation capacity.[5]

In the global budget, the largest source of inorganic chlorine gases (i.e., HCl and other inorganic chlorine gases, collectively defined as Cl_y) is the mobilization of chloride (Cl^-) from sea salt aerosol (SSA) through acid displacement by strong acids (H_2SO_4 and HNO_3).[6] Previous studies of tropospheric chlorine chemistry have focused on marine and coastal regions.[7–10] Most Cl_y species from marine sources deposit rapidly by wet scavenging,[11] and long-range transport to inland continental regions is unexpected. However, a study in a mid-continental region of North America far from the coast observed $ClNO_2$ production similar to that in coastal regions, highlighting the importance of Cl from non-SSA continental sources.[2, 12]. Observations and modeling suggest that reactive chlorine gaseous species in continental China are mainly from anthropogenic sources.[13, 14] High concentrations of particulate chlorine species have been observed in heavily polluted regions, such as the Indo-Gangetic Plain[1, 15, 16] and the North China Plain, [12, 17] indicating large emissions from anthropogenic sources. Greenland ice core measurements of excess Cl^- also highlight the possible direct chlorine emissions from anthropogenic sources.[18]

Tropospheric halogen chemistry has been a priority for several chemical transport models right through their various developmental stages.[6, 10, 19] The primary anthropogenic emissions of chlorine species, however, are not conventionally included in emission inventories, which hinders our understanding about the role of chlorine in the atmosphere. A few studies have developed regional chlorine emission inventories from anthropogenic sources,[20–22] based on emission factor measurements[23–25] and estimates of industrial and waste burning activities. The only available global chlorine emission inventory is the Reactive Chlorine Emission Inventory (RCEI) from 1990.[26–28] The coarse resolution (1°×1°) of this global inventory makes it challenging to study chlorine chemistry on finer scales, where it is most important and exerting impacts on regional to local scales. Several studies estimated the emissions from individual sectors, such as coal combustion,[29, 30] open waste burning,[31, 32] and biomass burning,[27] but these emissions are not consistent, indicating large uncertainties in current studies. Moreover, the long-term trends of chlorine emissions are unknown because most of these studies focused on emissions from a specific year.

In this study, we develop a global emission inventory of HCl and fine mode pCl based on an updated dataset of HCl and pCl emission factors (i.e., the amount of the pollutant emitted per unit activity conducted) and published state-of-the-art activity data. The activity data include Global Fire Emission Database (GFED4)[33] and the new historical biomass burning dataset for Coupled Model Intercomparison Project Phase 6 (BB4CMIP)[34] for biomass burning, PKU-FUEL[35] for energy, industrial and residential sectors, and a new estimate of waste burning developed in this study. We provide gridded, model-ready emission inventory at a high spatial resolution of 0.1° × 0.1° for the period from 1960 to 2014. Based on these data, we show the spatial and temporal patterns of HCl and pCl emissions and discuss their driving factors. Additionally, we discuss the atmospheric implications and potential future work.

2. Methods

In this study, we estimated the emissions from 6 sectors (i.e., energy production, industry, residence, open waste burning, open biomass burning, and agriculture). More detailed information including 13 subsectors and 35 sources which are summarized in Table 1. A bottom-up method was applied for country-level emission calculation, shown by Equation 1:

$$E = \sum_i E_i = \sum_i A_i \times EF_i \quad (1)$$

where E_i, A_i, and EF_i represent the emission rate (Gg Cl a^{-1}), activity data (Tg a^{-1}), and emission factor (g Cl kg^{-1}) from the *i*th source, respectively.

2.1 Activity data.

All activity data, except that for open waste burning, open biomass burning, and agricultural sectors, were taken from a published global high-resolution (0.1° × 0.1°) fuel consumption database PKU-FUEL.[35] The national-level fuel consumption data were mostly collected from International Energy Agency (IEA)[36] and a Chinese national questionnaire survey (for residential fuel consumption in China).[37, 38] Sub-national activity data were collected for large countries before spatial allocation. This procedure was conducted to reduce the uncertainty induced by the uneven distribution of per-capita energy consumption within these countries. The PKU-FUEL data is currently available from 1960 to 2014. Activity data of open biomass burning and agricultural burning processes were from Global Fire Emissions Database (GFED, Version 4.1)[33] (1997–2014) and historic biomass burning emissions for Coupled Model Intercomparison Project Phase 6 (BB4CMIP)[34] (1960 – 1997). Activity data of open waste burning was estimated based on the methods in the guidelines for estimating greenhouse gas (GHG) inventories provided by Intergovernmental Panel on Climate Change (IPCC) [39] with the data collected from the newest open-source datasets including OECD dataset[40], Eurostat[41], and Worldbank[42]. Detailed method and data source can be found in Text S1.

2.2 Emission factors.

Emissions factors from coal combustion processes were calculated based on chlorine content in coal (Tables S1, S2) and time-dependent removal efficiencies of air pollution control devices (APCDs; Tables S3, S4). Detailed information can be found in Text S2.1. Emissions factors from other processes in energy and industrial sectors except for coke production and brick production were calculated with fixed uncontrolled emission factors in the exhaust gas before entering the APCDs and the removal efficiency of APCDs (Table 1, Text S2.2). Emission factors for some industrial processes were calculated separately if more detailed EF data was available (such as coke production) or different assumptions of APCDs were made in these processes (such as brick production). Detailed information of those emission factors estimates can be found in Text S2.2. There were other industrial processes which might also need different assumptions, such as cement production, where the alkaline nature of cement can absorb acid gases like HCl and mitigate its emission. [43] We do not consider these differences in this study because of the lack of emission factor measurements, but we considered the uncertainty caused by emission factors using Monte Carlo simulations

described below (Section 2.5). Emission factors of open waste burning were calculated from chlorine content in different types of waste and the waste composition in different countries (Text S2.3). Emission factors of all sources in residential households (except coal combustion), as well as biomass and agricultural residue were collected from literature and kept constant along the study period (1960–2014) (Table 1).

2.3 Spatial allocation.

Gridded, model-ready, emissions for industrial, residential, and energy sectors (i.e., with activity data from PKU-FUEL) were derived by multiplying emission factors to the high-resolution activity data, which was gridded to a 0.1° × 0.1° (approximately 10 × 10 km) grid using proxies such as locations of the industry and power plants (for energy and industrial sectors), and population (for other sectors, such as residential).[35] Emissions from energy and industrial sectors were equally allocated to each month. Emissions from residential households were allocated to each month using grid-specific monthly profiles from a previous study.[54] Gridded emissions from open biomass burning and agricultural processes were calculated by regridding the activity data from GFED4/BB4CMIP on a 0.25° × 0.25° grid with monthly profiles onto a 0.1° × 0.1° grid using the python package ESMPy to perform regridding that is conservative for the total emission. Gridded emissions from open waste burning were allocated to a 0.1° × 0.1° grid based on regridded population and urban-rural population percentage assuming equal distribution in each month, as described in Text S1.

2.4 Decomposition of the driving factors for temporal changes of HCl and pCl emissions.

To study the driving factors of HCl and pCl emission trends, we divided the study period into five decades (i.e., 1960–1970, 1970–1980, 1980–1990, 1990–2000, 2000–2010), and calculated the emission difference between the end year and the start year of each decade. Then we decomposed the emission differences into four indices that might affect emissions, including the emission factor (EF), the emission intensity (EI, calculated by fuel consumption/gross domestic product (GDP)), economic development (ECO, represented by GDP per capita), and population (POP) based on a logarithmic mean Divisia index (LMDI) approach[55, 56]. The detailed method description can be found in Text S3. We nominally applied this method for anthropogenic processes, such as emissions from power plants, industries, residences, and open waste burning. Emissions from open biomass burning were not considered since it was affected more by wildfires, which were controlled by different processes.

2.5 Uncertainty analysis.

We used Monte Carlo simulations to evaluate the uncertainty of this emission inventory by running 10,000 simulations with random input values drawn from the uncertainty distributions of input variables. The emission factors were assumed to follow log-normal distributions, following previous studies.[57–59] Activity data (except for open waste burning), population data and other parameters were assumed to be uniformly distributed. The uncertainties of activity data were set to be 5% for fuel consumption in energy and industrial sectors, 20% for residential sectors and open biomass burning, following previous studies.[57–59] The uncertainty of emission factors was represented by the standard deviation

of log-transformed values of multiple records are available for the same processes in Table 1, otherwise we assume the uncertainty to be 50%. The uncertainty of population data was set to be 20%, and the uncertainty of other parameters (e.g., chlorine content) was set to be 50%. The uncertainty of activity data of open waste burning was calculated by aggregating the uncertainties of all the parameters described in Text S1. The uncertainty of emissions was represented by the interquartile range (IQR; i.e., the interval between the 25th and 75th percentiles) throughout the text.

3. Results and discussion

3.1 HCl and particulate Cl emissions by sectors in 2014

Our analyses focus on the emissions in 2014 because it is the most recent year with comprehensive activity data available in our study. In 2014, the estimated emissions of HCl and pCl are 2354 Gg Cl a^{-1} (IQR: 1661 – 3200 Gg Cl a^{-1}) and 2321 Gg Cl a^{-1} (IQR: 930 – 3264 Gg Cl a^{-1}), respectively, leading to a total Cl (tCl = HCl + pCl) emission of 4675 Gg Cl a^{-1} (IQR: 2591 – 6464 Gg Cl a^{-1}, Table 2). Most of the emissions are from Africa and Asia (including China and other Asian countries), while emissions from other regions are relatively small, contributing to less than 30% of world total emissions for both HCl and pCl (Figure 1). The three countries that emit the most HCl are China, India, and the US, contributing 42% of the global total. The three countries that emit the most pCl are India, China, and Russia, emitting 24% of the global total (Figure S1). Overall, China is the country that emits the most tCl (913 Gg Cl a^{-1} of tCl in 2014), followed by India (371 Gg Cl a^{-1} of total Cl in 2014).

Although our estimates show that the magnitudes of global HCl and pCl emissions are comparable, the major sources are different (Figure 1). HCl emissions are mostly from open waste burning (38%), open biomass burning (19%), energy (19%) and residential (13%) sectors, although the major source sectors are variable for different countries (Figure S1). Major emission sources of HCl classified by the types of fuel are waste, biomass, and coal, which contribute 43%, 32%, and 25% of the total HCl emission, respectively. On the contrary, pCl emissions are mainly emitted from the open biomass burning (44%), residential (29%), and agricultural sectors (16%), and the combustion of biomass/biofuel contributes 90% of the total (Figure 1). Such differences in sectoral emission profiles of HCl and pCl are mainly caused by differences in emission factors. For example, in coal combustion, higher conversion ratio of released Cl to HCl than that to pCl (88% vs. 9%),[60] together with higher removal efficiency of particulate matter than acidic gases (discussed in Text S2), favor the emission of HCl relative to pCl. For most types of biomasses, emission factors of pCl are higher than those of HCl (Table 1). The differences in major sources have implications on future trends and pollution control strategies. Emissions of HCl will likely be reduced in the future because the major sources are power plants and industry (contributing to 43% of total emissions), which can be further reduced by higher installation rate and higher removal efficiency of APCDs. On the contrary, 90% of pCl are emitted from uncontrolled combustion processes, such as indoor biofuel burning and open biomass burning. Further emissions reductions will rely more on the shift of residential energy use towards cleaner energy, such as natural gas and electricity.

3.2. Spatial distributions

Figure 2 shows the spatial distributions of HCl and pCl emissions from all sources in 2014 at a spatial resolution of 0.1° × 0.1°. The spatial distributions from each sector are shown in Figure S2. As a caveat, emissions from a few African countries might be underestimated, because the activity data in some energy sectors (e.g., coal and solid waste) are not available. The overall spatial distributions of HCl and pCl are similar, both mainly driven by combustion processes, though in some areas the spatial patterns are different because of differences in emission factors. In general, high emissions of HCl and pCl collocate with high emissions of other major air pollutants such as $PM_{2.5}$, CO_2, SO_2, and NO_x (NO + NO_2) in populated regions, [35, 57, 59, 61] such as eastern and southern Asia, Europe, and the eastern US. Other areas associated with moderate emissions of most air pollutants show high HCl and pCl emissions, such as Africa and Latin America, where emissions from biomass burning contribute more than half of the tCl emissions.

The major sources of HCl vary among different regions as shown in the pie charts in Figure 2 (a). For example, in China, the major source is open waste burning, which accounts for 46% of a total HCl emission of 705 Gg Cl a^{-1} in 2014. These values can be compared with a previous study showing that 41% out of 458 Gg a^{-1} HCl is emitted from waste burning in China in 2014[20] (Table S3). Open waste burning is also the major HCl source in other Asian countries (32%, Figure 2). High emissions from open waste burning, especially in China, India, and other Asian countries, are attributable to the high population and a developing economy, resulting in an increasing amount of waste production and a high fraction of uncollected waste that is openly burnt.[32] Emissions from industrial sectors in China are also high, mainly because of high HCl emissions from coal combustion processes such as brick production, as bricks production in China contributes to 67% of the world total. [62] In Europe, the largest sources of HCl are from the energy and open waste burning sectors, which account for 38% and 23% of the total HCl emissions in 2014, respectively. For the energy sector, the main sources of HCl classified based on types of fuels are coal combustion (23%) and waste incineration (14%). Because of the relatively high cost, waste incineration is mainly used in Europe, Japan, the U.S., and China.[63] Emissions from this source are relatively more important in Europe compared with other regions, because of the lack of other sources. Emissions from the energy sector are more prominent in North America, contributing to 43% of total HCl emissions, because of the high dependency of energy generation on coal combustion and wide use of waste incineration for energy recovery.

The pCl emissions are almost exclusively from biomass and biofuel burning processes, including open biomass burning (44% in 2014), indoor biofuel burning (29%), and open burning of agricultural residue (16%). Open biomass burning, such as wildfires, contributes 88%, 67%, 63%, 56% of pCl emissions in Oceania, Latin America, Africa, and North America, respectively. High emissions mainly occur in large areas with vegetation such as savannah and grasslands in Africa, forest in South America, and boreal regions of Europe and Asia, where fire activities are high as indicated by the GFED4 dataset. High emissions from the residential sector are usually located in densely populated areas in developing countries, such as India, eastern China, and some African countries, and most of the

emissions in this sector are from indoor biofuel burning that could lead to direct exposure by residents.[64]

3.3. The temporal variation and its driving factors

Historical trends of HCl, pCl and total Cl emissions are shown in Figure 3 for different source sectors (upper panels) and different regions (lower panels). The global chlorine emission in the form of HCl increases from 1786 Gg Cl a^{-1} in 1960 to a peak of 2678 Gg Cl a^{-1} in 1990s and shows reduction thereafter to 2354 Gg Cl a^{-1} in 2014. For the global emission of pCl, a small increase from 1915 to 2271 Gg Cl a^{-1} can be seen from 1960s to 1980s, and the value is relatively stable afterward, except a peak in 1998, caused by the large emission from wildfires in Indonesia. Though HCl and pCl emissions in 1960 and 2014 are very similar, the sectoral and regional distributions are different (Table 2). HCl and pCl emission trends are mainly driven by changes in sectors related to anthropogenic processes, i.e., energy, industrial, residential, and open waste burning sectors, while emissions from wildfires and other biomass burning fluctuate around a relatively constant level, as suggested by BB4CMIP. We further delineate factors that drive temporal variations in emissions from the aforementioned anthropogenic sectors by calculating the contributions of four related indices (i.e., EF, EI, ECO, POP) over five decades using a decomposition method (Section 2.4 and Text S3). Our results indicate that economic and population growths are driving the increases in HCl and pCl emissions. However, these increases are largely compensated for by decreases in emission factors and emission intensities, particularly in energy production and industry (Figure 4).

For HCl emissions, energy is the major sector from 1960s to 1980s (Figure 3), because of the large emission increase in this period, especially in Europe (Figures S3 and S4). The rapid increase in the energy sector is likely driven by the increasing use of fossil fuels in power plants, where the contributions of energy intensity and economy have the largest positive contribution to emission increase during this period (Figure S5). APCDs had not been widely adopted in most countries until the 1980s,[65] and the contribution of emission factor changes, which reflects the use of APCDs, only have a small effect in cutting down emissions (Figure S5). After wide adoption of APCDs, especially in the largest HCl emission region in Europe, emissions in energy sectors are reduced after the 1980s (Figures S3 and S4). The HCl emission trend for the industrial sector has a peak in 1990s, driven by the increase of emissions in developing countries, especially in China, mainly from coal combustion in industrial processes (Figure S4). Emissions from residential sectors are relatively constant during the study period, as the decrease in residential coal combustion emissions from European countries offsets the increase of indoor biofuel combustion emissions in Asian countries (Figure S4). Emission from open waste burning increased in all regions during the study period mainly caused by developing economies and population growth (Figures S4 and S5). Both factors increase the amount of waste burned and this increasing trend will likely continue. Since emissions from energy and industrial sectors show decreasing trends, the rising emissions of HCl from the residential sector, especially indoor biofuel burning in developing countries, and the open waste burning sector, might become more important in the future and require special attention from policymakers.

Emissions of pCl from energy, industrial, and open waste burning sectors exhibit qualitatively similar trends to that of HCl but quantitatively the magnitude of variations are much smaller (Figure 3). Thus, the overall emission trend of pCl is dominated by the relatively steady emissions from open biomass burning, most of which are from Africa due to frequent wildfire, and a small increase in emissions from residential sectors (Figures 3 and S4). Emissions from the residential sector, especially that from indoor biofuel burning, are the largest anthropogenic sources of pCl, mainly emitted from African and Asian countries (Figure S4), where biofuel is one of the main fuel types for households in these regions.[66, 67] Emissions from Africa and Asia are increasing during the study period, because of the increasing population and growing economy (Figure S5), while emissions from China started to decrease from 1990 (Figure 3), likely due to wider use of cleaner energy in households (e.g. liquid petroleum gas and biogas).[37] Anthropogenic emissions of pCl are much smaller and less important in other regions, i.e., Europe, North America, Latin America, and Oceania (Figure 3).

3.4. Comparison with emission trends of other aerosol precursors

We compare the trends of tCl calculated in this study with other common pollutants including SO_2, NO_x, and NH_3 estimated by adding up anthropogenic emissions from the Community Emissions Data System (CEDS),[68–70] open biomass burning and agricultural residue burning from BB4CMIP[34] (Figure 5). These species are major precursors for inorganic aerosol formation. Emissions of tCl and SO_2 increase over the period from 1960 to 1990 and decrease afterward, which are mainly caused by the wide application of APCDs that reduce acid gas emissions from energy and industrial sectors. However, further control of tCl emission could be more challenging than SO_2, because a large fraction of tCl emissions is from open biomass burning and the residential sector (Section 3.3). Compared with the rapid reduction of SO_2, a slower reduction rate is observed for tCl emission in the last two decades. Emissions of NO_x remain increased after the 1990s and stabilize in recent years, which is a result of a decreasing trend of emissions in Europe and North America offset by the increasing trend in Asian countries.[69] Emissions of NH_3 continually increase due to increasing trends in the agricultural sector driven by a growing population.

Although we estimate HCl and pCl emissions separately, these species can undergo gas-particle partitioning processes in the atmosphere. Thermodynamic modeling suggests that the particulate fraction of chloride largely depends on temperature, aerosol water, and the abundance of ammonia, and the gaseous HCl can co-condense with aerosol water into the particulate phase during haze events, particularly in cold, humid conditions in polluted regions.[1] The increase in NH_3 is favorable for chloride to partition into the particle phase, while the decrease in SO_2 and sulfate may reduce aerosol water, which drives the chloride to partition into the gas phase. Further chemical transport modeling and thermodynamic modeling studies are needed to better understand the effect of changing emission profiles on inorganic aerosol compositions.

3.5. Uncertainties and comparison with regional emissions in literature

We compare our results with emissions from other studies, including the worldwide 1990 RECI emission inventory[26] and the 2014 emission inventory in China,[20] as well as other

available regional and sectoral emission estimates (Text S4 and Table S6). Most of our results are within the reported uncertainty range. However, the uncertainty estimates using Monte Carlo simulations indicate that there are relatively large uncertainties in our results (−29% to 36% for HCl and −60% to 41% for pCl, Table 2), higher than other emission inventories developed based on the PKU-FUEL dataset.[35, 57, 59, 61] A detailed discussion of the uncertainty and comparison can be found in the supplementary information (Text S4).

There are large inevitable uncertainties in the estimation of some parameters (such as APCD installation rates in coal combustion processes, waste production and collection rate in open waste burning), especially in the early years, due to a lack of records. Also, the chlorine content of coal, waste, and biomass vary significantly with different locations, causing emission factors to vary in different studies. However, the uncertainties can still be reduced, and the study can be improved in some ways. First, more measurements are needed to obtain more accurate emission factors, especially for processes with large emissions, such as burning processes of different types of biomasses (both indoor and open burning), combustion of coal from different regions. Activity data of open waste burning needs to be further studied because emissions from this sector are increasingly important (Figure 3). For example, emissions of HCl in this sector gradually exceed emissions from other major sources (i.e., energy and industrial sectors) in China, other Asian countries and Africa (Figure S3).

4. Atmospheric implications and future work

This study provides an estimate of the global continental emissions of HCl and pCl from 1960 to 2014 at a fine spatial resolution (0.1° × 0.1°). Our results can be used to study tropospheric chlorine chemistry in global and regional chemical transport models. Continental emissions of HCl and pCl can be potentially important for the nighttime $ClNO_2$ production by reactive uptake of N_2O_5 on chloride aerosol particles. The photolysis of $ClNO_2$ in the morning can produce chlorine radical (Cl·), which reacts rapidly with VOCs to affect ozone and SOA formation. Our study implies that these reactions are not limited to coastal regions (where both NO_x and sea salt chloride are abundant), as continental emissions of HCl and pCl can also serve as an important source of chloride aerosol. The role of continental chlorine emissions on tropospheric oxidation capacity should be further examined.

Our study highlights high emissions of HCl and pCl in populated regions such as the North China Plain and Indo-Gangetic Plain, consistent with field observations showing high chloride concentrations in the particulate matter.[1, 12, 71, 72] As we mainly focus on emissions from combustion processes in this study, future work should also examine HCl and pCl from non-combustion processes. For example, high concentrations of $ClNO_2$ and elevated particulate Cl^- observed in snowy urban areas during wintertime suggest the contribution of road salt for deicing purposes could be an important source.[73–75] The consumption of acid solution in metal pickling industry can also be a direct source of HCl in Delhi, India suggested by previous field observations.[15, 76] The magnitude and importance of these emissions remain largely unclear.

Besides HCl and pCl, other forms of chlorine emitted from anthropogenic sources, such as Cl_2 and HOCl, although beyond the scope of this work, may also play an important role in tropospheric chemistry because they are also important Cl· precursors. State-level or county-level emissions of Cl_2 and HOCl have been estimated in some studies, such as in the U.S.,[77, 78] China,[79, 80] and these studies found that the major sources could be biocides used in cooling towers, disinfectants in wastewater treatment plants and swimming pools. Previous studies mentioned above only estimated state-level or city-level emissions, to compare with country-level HCl and pCl emissions in this study, we did a rough estimation by assuming emissions per capita are the same in the whole country and multiplying the regional emissions by the national-to-regional population ratio. This leads to 20 – 131 Gg Cl a^{-1} in the U.S. and 12 – 493 Gg Cl a^{-1} in China emitted in the form of Cl_2 or HOCl. The upper limit estimates could be comparable to HCl emissions calculated in this study (i.e., 94 Gg Cl a^{-1} in the U.S. and 705 Gg Cl a^{-1} in China). Although this is a rough estimate based on limited information, this indicates the potential importance of HOCl and Cl_2 emissions. We recommend further studies on estimating these emissions and model simulations to study their effects on atmospheric chemistry.

Supplementary Material

Refer to Web version on PubMed Central for supplementary material.

Acknowledgments

This study is supported by P. L.'s start-up funding from Georgia Institute of Technology. The development of PKU-FUEL is supported by the National Natural Science Foundation of China (Grants 41991312, 41830641, 41922057, and 41821005), Chinese Academy of Science (XDA23010100), Ministry of Science and Technology of the People's Republic of China (2019QZKK0605), and Center for Computational Science and Engineering at Southern University of Science and Technology. Part of this work is funded by the U.S. Environmental Protection Agency (EPA grant number R835880), and the National Science Foundation (NSF SRN grant number 1444745). Its contents are solely the responsibility of the grantee and do not necessarily represent the official views of the supporting agencies. Further, the US government does not endorse the purchase of any commercial products or services mentioned in the publication.

References

1. Gunthe SS; Liu P; Panda U; Raj SS; Sharma A; Darbyshire E; Reyes-Villegas E; Allan J; Chen Y; Wang X; Song S; Pöhlker ML; Shi L; Wang Y; Kommula SM; Liu T; Ravikrishna R; McFiggans G; Mickley LJ; Martin ST; Pöschl U; Andreae MO; Coe H, Enhanced aerosol particle growth sustained by high continental chlorine emission in India. Nature Geoscience 2021, 14, (2), 77–84.
2. Thornton JA; Kercher JP; Riedel TP; Wagner NL; Cozic J; Holloway JS; Dubé WP; Wolfe GM; Quinn PK; Middlebrook AM; Alexander B; Brown SS, A large atomic chlorine source inferred from mid-continental reactive nitrogen chemistry. Nature 2010, 464, (7286), 271–274. [PubMed: 20220847]
3. Choi MS; Qiu X; Zhang J; Wang S; Li X; Sun Y; Chen J; Ying Q, Study of Secondary Organic Aerosol Formation from Chlorine Radical-Initiated Oxidation of Volatile Organic Compounds in a Polluted Atmosphere Using a 3D Chemical Transport Model. Environmental Science & Technology 2020, 54, (21), 13409–13418. [PubMed: 33074656]
4. Cai X; Griffin RJ, Secondary aerosol formation from the oxidation of biogenic hydrocarbons by chlorine atoms. Journal of Geophysical Research: Atmospheres 2006, 111, (D14).
5. Zhang R; Gen M; Huang D; Li Y; Chan CK, Enhanced Sulfate Production by Nitrate Photolysis in the Presence of Halide Ions in Atmospheric Particles. Environmental Science & Technology 2020, 54, (7), 3831–3839. [PubMed: 32126769]

6. Wang X; Jacob DJ; Eastham SD; Sulprizio MP; Zhu L; Chen Q; Alexander B; Sherwen T; Evans MJ; Lee BH; Haskins JD; Lopez-Hilfiker FD; Thornton JA; Huey GL; Liao H, The role of chlorine in global tropospheric chemistry. Atmos. Chem. Phys 2019, 19, (6), 3981–4003.
7. Pechtl S; von Glasow R, Reactive chlorine in the marine boundary layer in the outflow of polluted continental air: A model study. Geophysical Research Letters 2007, 34, (11).
8. Riedel TP; Bertram TH; Crisp TA; Williams EJ; Lerner BM; Vlasenko A; Li S-M; Gilman J; de Gouw J; Bon DM; Wagner NL; Brown SS; Thornton JA, Nitryl Chloride and Molecular Chlorine in the Coastal Marine Boundary Layer. Environmental Science & Technology 2012, 46, (19), 10463–10470. [PubMed: 22443276]
9. Knipping EM; Dabdub D, Impact of Chlorine Emissions from Sea-Salt Aerosol on Coastal Urban Ozone. Environmental Science & Technology 2003, 37, (2), 275–284. [PubMed: 12564898]
10. Li Q; Borge R; Sarwar G; de la Paz D; Gantt B; Domingo J; Cuevas CA; Saiz-Lopez A, Impact of halogen chemistry on summertime air quality in coastal and continental Europe: application of the CMAQ model and implications for regulation. Atmos. Chem. Phys 2019, 19, (24), 15321–15337. [PubMed: 32425994]
11. Pio CA; Lopes DA, Chlorine loss from marine aerosol in a coastal atmosphere. Journal of Geophysical Research: Atmospheres 1998, 103, (D19), 25263–25272.
12. Yang X; Wang T; Xia M; Gao X; Li Q; Zhang N; Gao Y; Lee S; Wang X; Xue L; Yang L; Wang W, Abundance and origin of fine particulate chloride in continental China. Science of The Total Environment 2018, 624, 1041–1051. [PubMed: 29929221]
13. Wang X; Jacob DJ; Fu X; Wang T; Breton ML; Hallquist M; Liu Z; McDuffie EE; Liao H, Effects of Anthropogenic Chlorine on PM2.5 and Ozone Air Quality in China. Environmental Science & Technology 2020, 54, (16), 9908–9916. [PubMed: 32600027]
14. Liu X; Qu H; Huey LG; Wang Y; Sjostedt S; Zeng L; Lu K; Wu Y; Hu M; Shao M; Zhu T; Zhang Y, High Levels of Daytime Molecular Chlorine and Nitryl Chloride at a Rural Site on the North China Plain. Environmental Science & Technology 2017, 51, (17), 9588–9595. [PubMed: 28806070]
15. Gani S; Bhandari S; Seraj S; Wang DS; Patel K; Soni P; Arub Z; Habib G; Hildebrandt Ruiz L; Apte JS, Submicron aerosol composition in the world's most polluted megacity: the Delhi Aerosol Supersite study. Atmos. Chem. Phys 2019, 19, (10), 6843–6859.
16. Bhandari S; Gani S; Patel K; Wang DS; Soni P; Arub Z; Habib G; Apte JS; Hildebrandt Ruiz L, Sources and atmospheric dynamics of organic aerosol in New Delhi, India: insights from receptor modeling. Atmos. Chem. Phys 2020, 20, (2), 735–752.
17. Song S; Nenes A; Gao M; Zhang Y; Liu P; Shao J; Ye D; Xu W; Lei L; Sun Y; Liu B; Wang S; McElroy MB, Thermodynamic Modeling Suggests Declines in Water Uptake and Acidity of Inorganic Aerosols in Beijing Winter Haze Events during 2014/2015–2018/2019. Environmental Science & Technology Letters 2019, 6, (12), 752–760.
18. Zhai S; Wang X; McConnell JR; Geng L; Cole-Dai J; Sigl M; Chellman N; Sherwen T; Pound R; Fujita K; Hattori S; Moch JM; Zhu L; Evans M; Legrand M; Liu P; Pasteris D; Chan Y-C; Murray LT; Alexander B, Anthropogenic Impacts on Tropospheric Reactive Chlorine since the Preindustrial. Geophysical Research Letters 2021, n/a, (n/a), e2021GL093808.
19. Li Q; Badia A; Wang T; Sarwar G; Fu X; Zhang L; Zhang Q; Fung J; Cuevas CA; Wang S; Zhou B; Saiz-Lopez A, Potential Effect of Halogens on Atmospheric Oxidation and Air Quality in China. Journal of Geophysical Research: Atmospheres 2020, 125, (9), e2019JD032058.
20. Fu X; Wang T; Wang S; Zhang L; Cai S; Xing J; Hao J, Anthropogenic Emissions of Hydrogen Chloride and Fine Particulate Chloride in China. Environmental Science & Technology 2018, 52, (3), 1644–1654. [PubMed: 29376646]
21. Tian H; Gao J; Lu L; Zhao D; Cheng K; Qiu P, Temporal Trends and Spatial Variation Characteristics of Hazardous Air Pollutant Emission Inventory from Municipal Solid Waste Incineration in China. Environmental Science & Technology 2012, 46, (18), 10364–10371. [PubMed: 22920612]
22. Tian H; Liu K; Zhou J; Lu L; Hao J; Qiu P; Gao J; Zhu C; Wang K; Hua S, Atmospheric Emission Inventory of Hazardous Trace Elements from China's Coal-Fired Power Plants—Temporal Trends

and Spatial Variation Characteristics. Environmental Science & Technology 2014, 48, (6), 3575–3582. [PubMed: 24564872]

23. Ding X; Li Q; Wu D; Huo Y; Liang Y; Wang H; Zhang J; Wang S; Wang T; Ye X; Chen J, Gaseous and Particulate Chlorine Emissions From Typical Iron and Steel Industry in China. Journal of Geophysical Research: Atmospheres 2020, 125, (15), e2020JD032729.
24. Lee BH; Lopez-Hilfiker FD; Schroder JC; Campuzano-Jost P; Jimenez JL; McDuffie EE; Fibiger DL; Veres PR; Brown SS; Campos TL; Weinheimer AJ; Flocke FF; Norris G; O'Mara K; Green JR; Fiddler MN; Bililign S; Shah V; Jaeglé L; Thornton JA, Airborne Observations of Reactive Inorganic Chlorine and Bromine Species in the Exhaust of Coal-Fired Power Plants. Journal of Geophysical Research: Atmospheres 2018, 123, (19), 11,225–11,237.
25. Akagi SK; Yokelson RJ; Wiedinmyer C; Alvarado MJ; Reid JS; Karl T; Crounse JD; Wennberg PO, Emission factors for open and domestic biomass burning for use in atmospheric models. Atmos. Chem. Phys 2011, 11, (9), 4039–4072.
26. McCulloch A; Aucott ML; Benkovitz CM; Graedel TE; Kleiman G; Midgley PM; Li Y-F, Global emissions of hydrogen chloride and chloromethane from coal combustion, incineration and industrial activities: Reactive Chlorine Emissions Inventory. Journal of Geophysical Research: Atmospheres 1999, 104, (D7), 8391–8403.
27. Lobert JM; Keene WC; Logan JA; Yevich R, Global chlorine emissions from biomass burning: Reactive Chlorine Emissions Inventory. Journal of Geophysical Research: Atmospheres 1999, 104, (D7), 8373–8389.
28. Khalil MAK; Moore RM; Harper DB; Lobert JM; Erickson DJ; Koropalov V; Sturges WT; Keene WC, Natural emissions of chlorine-containing gases: Reactive Chlorine Emissions Inventory. Journal of Geophysical Research: Atmospheres 1999, 104, (D7), 8333–8346.
29. Liu F; Zhang Q; Tong D; Zheng B; Li M; Huo H; He KB, High-resolution inventory of technologies, activities, and emissions of coal-fired power plants in China from 1990 to 2010. Atmos. Chem. Phys 2015, 15, (23), 13299–13317.
30. Liu Y; Fan Q; Chen X; Zhao J; Ling Z; Hong Y; Li W; Chen X; Wang M; Wei X, Modeling the impact of chlorine emissions from coal combustion and prescribed waste incineration on tropospheric ozone formation in China. Atmos. Chem. Phys 2018, 18, (4), 2709–2724.
31. Sharma G; Sinha B; Pallavi; Hakkim H; Chandra BP; Kumar A; Sinha V, Gridded Emissions of CO, NOx, SO2, CO2, NH3, HCl, CH4, PM2.5, PM10, BC, and NMVOC from Open Municipal Waste Burning in India. Environmental Science & Technology 2019, 53, (9), 4765–4774. [PubMed: 31021611]
32. Wiedinmyer C; Yokelson RJ; Gullett BK, Global Emissions of Trace Gases, Particulate Matter, and Hazardous Air Pollutants from Open Burning of Domestic Waste. Environmental Science & Technology 2014, 48, (16), 9523–9530. [PubMed: 25019173]
33. van der Werf GR; Randerson JT; Giglio L; van Leeuwen TT; Chen Y; Rogers BM; Mu M; van Marle MJE; Morton DC; Collatz GJ; Yokelson RJ; Kasibhatla PS, Global fire emissions estimates during 1997–2016. Earth Syst. Sci. Data 2017, 9, (2), 697–720.
34. van Marle MJE; Kloster S; Magi BI; Marlon JR; Daniau AL; Field RD; Arneth A; Forrest M; Hantson S; Kehrwald NM; Knorr W; Lasslop G; Li F; Mangeon S; Yue C; Kaiser JW; van der Werf GR, Historic global biomass burning emissions for CMIP6 (BB4CMIP) based on merging satellite observations with proxies and fire models (1750–2015). Geosci. Model Dev 2017, 10, (9), 3329–3357.
35. Wang R; Tao S; Ciais P; Shen HZ; Huang Y; Chen H; Shen GF; Wang B; Li W; Zhang YY; Lu Y; Zhu D; Chen YC; Liu XP; Wang WT; Wang XL; Liu WX; Li BG; Piao SL, High-resolution mapping of combustion processes and implications for CO2 emissions. Atmos. Chem. Phys 2013, 13, (10), 5189–5203.
36. International Energy Agency, IEA World Energy Statistics and Balances. In https://www.oecd-ilibrary.org/statistics.
37. Tao S; Ru MY; Du W; Zhu X; Zhong QR; Li BG; Shen GF; Pan XL; Meng WJ; Chen YL; Shen HZ; Lin N; Su S; Zhuo SJ; Huang TB; Xu Y; Yun X; Liu JF; Wang XL; Liu WX; Cheng HF; Zhu DQ, Quantifying the rural residential energy transition in China from 1992 to 2012 through a representative national survey. Nature Energy 2018, 3, (7), 567–573.

38. Zhu X; Yun X; Meng W; Xu H; Du W; Shen G; Cheng H; Ma J; Tao S, Stacked Use and Transition Trends of Rural Household Energy in Mainland China. Environmental Science & Technology 2019, 53, (1), 521–529. [PubMed: 30512946]
39. IPCC, 2006 IPCC Guidelines for National Greenhouse Gas Inventories IGES, Japan 2006.
40. OECD, Municipal waste, Generation and Treatment In https://stats.oecd.org/Index.aspx?DataSetCode=MUNW.
41. Eurostat, Municipality waste statistics. In Eurostat, Ed. http://appsso.eurostat.ec.europa.eu/nui/show.do?dataset=env_wasmun.
42. Kaza S; Yao LC; Bhada-Tata P; Van Woerden F, What a Waste 2.0 : A Global Snapshot of Solid Waste Management to 2050. Urban Development;. Washington, DC: World Bank: 2018.
43. U.S. EPA, AP-42, Chapter 11: Mineral Products Industry. In Fifth ed.; https://www3.epa.gov/ttnchie1/ap42/ch11/final/c11s06.pdf, 2014; Vol. 1.
44. U.S. EPA, AP-42, Chapter 2: Solid Waste Disposal. In Fifth ed.; https://www3.epa.gov/ttnchie1/ap42/ch02/, 2014; Vol. 1.
45. Reff A; Bhave PV; Simon H; Pace TG; Pouliot GA; Mobley JD; Houyoux M, Emissions Inventory of PM2.5 Trace Elements across the United States. Environmental Science & Technology 2009, 43, (15), 5790–5796. [PubMed: 19731678]
46. Andreae MO, Emission of trace gases and aerosols from biomass burning – an updated assessment. Atmos. Chem. Phys 2019, 19, (13), 8523–8546.
47. Andreae MO, Biomass Burning Emission factors. In Max Planck Society, Ed. 10.17617/3.26, 2019.
48. Christian TJ; Yokelson RJ; Cárdenas B; Molina LT; Engling G; Hsu SC, Trace gas and particle emissions from domestic and industrial biofuel use and garbage burning in central Mexico. Atmos. Chem. Phys 2010, 10, (2), 565–584.
49. Lemieux P. EVALUATION OF EMISSIONS FROM THE OPEN BURNING OF HOUSEHOLD WASTE IN BARRELS - VOLUME 1. TECHNICAL REPORT; EPA/600/R-97/134b; U.S. Environmental Protection Agency: Research Triangle, NC., 1997.
50. Stockwell CE; Christian TJ; Goetz JD; Jayarathne T; Bhave PV; Praveen PS; Adhikari S; Maharjan R; DeCarlo PF; Stone EA; Saikawa E; Blake DR; Simpson IJ; Yokelson RJ; Panday AK, Nepal Ambient Monitoring and Source Testing Experiment (NAMaSTE): emissions of trace gases and light-absorbing carbon from wood and dung cooking fires, garbage and crop residue burning, brick kilns, and other sources. Atmos. Chem. Phys 2016, 16, (17), 11043–11081.
51. Yokelson RJ; Burling IR; Urbanski SP; Atlas EL; Adachi K; Buseck PR; Wiedinmyer C; Akagi SK; Toohey DW; Wold CE, Trace gas and particle emissions from open biomass burning in Mexico. Atmos. Chem. Phys 2011, 11, (14), 6787–6808.
52. Keene WC; Lobert JM; Crutzen PJ; Maben JR; Scharffe DH; Landmann T; Hély C; Brain C, Emissions of major gaseous and particulate species during experimental burns of southern African biomass. Journal of Geophysical Research: Atmospheres 2006, 111, (D4).
53. Wang J; Niu X; Sun J; Zhang Y; Zhang T; Shen Z; Zhang Q; Xu H; Li X; Zhang R, Source profiles of PM2.5 emitted from four typical open burning sources and its cytotoxicity to vascular smooth muscle cells. Science of The Total Environment 2020, 715, 136949. [PubMed: 32041051]
54. Chen H; Huang Y; Shen H; Chen Y; Ru M; Chen Y; Lin N; Su S; Zhuo S; Zhong Q; Wang X; Liu J; Li B; Tao S, Modeling temporal variations in global residential energy consumption and pollutant emissions. Applied Energy 2016, 184, 820–829.
55. Ang BW, LMDI decomposition approach: A guide for implementation. Energy Policy 2015, 86, 233–238.
56. Madaleno M; Moutinho V, A new LDMI decomposition approach to explain emission development in the EU: individual and set contribution. Environmental Science and Pollution Research 2017, 24, (11), 10234–10257. [PubMed: 28265876]
57. Huang Y; Shen H; Chen H; Wang R; Zhang Y; Su S; Chen Y; Lin N; Zhuo S; Zhong Q; Wang X; Liu J; Li B; Liu W; Tao S, Quantification of Global Primary Emissions of PM2.5, PM10, and TSP from Combustion and Industrial Process Sources. Environmental Science & Technology 2014, 48, (23), 13834–13843. [PubMed: 25347079]

58. Shen H; Huang Y; Wang R; Zhu D; Li W; Shen G; Wang B; Zhang Y; Chen Y; Lu Y; Chen H; Li T; Sun K; Li B; Liu W; Liu J; Tao S, Global Atmospheric Emissions of Polycyclic Aromatic Hydrocarbons from 1960 to 2008 and Future Predictions. Environmental Science & Technology 2013, 47, (12), 6415–6424. [PubMed: 23659377]
59. Zhong Q; Shen H; Yun X; Chen Y; Ren Y. a.; Xu H; Shen G; Du W; Meng J; Li W; Ma J; Tao S, Global Sulfur Dioxide Emissions and the Driving Forces. Environmental Science & Technology 2020, 54, (11), 6508–6517. [PubMed: 32379431]
60. Deng S; Zhang C; Liu Y; Cao Q; Xu Y; Wang H; Zhang F, A full-scale field study on chlorine emission of pulverized coal-fired power plants in China. Environmental Research Study 2014, 27, (02), 127–133.
61. Huang T; Zhu X; Zhong Q; Yun X; Meng W; Li B; Ma J; Zeng EY; Tao S, Spatial and Temporal Trends in Global Emissions of Nitrogen Oxides from 1960 to 2014. Environmental Science & Technology 2017, 51, (14), 7992–8000. [PubMed: 28613845]
62. Eil A; Li J; Baral P; Saikawa E. DIRTY STACKS, HIGH STAKES: An Overview of Brick Sector in South Asia; 2020.
63. Scarlat N; Fahl F; Dallemand J-F, Status and Opportunities for Energy Recovery from Municipal Solid Waste in Europe. Waste and Biomass Valorization 2019, 10, (9), 2425–2444.
64. Begum BA; Paul SK; Dildar Hossain M; Biswas SK; Hopke PK, Indoor air pollution from particulate matter emissions in different households in rural areas of Bangladesh. Building and Environment 2009, 44, (5), 898–903.
65. Mylona S, Sulphur dioxide emissions in Europe 1880–1991 and their effect on sulphur concentrations and depositions. Tellus B 1996, 48, (5), 662–689.
66. Mohammed YS; Bashir N; Mustafa MW, Overuse of wood-based bioenergy in selected sub-Saharan Africa countries: review of unconstructive challenges and suggestions. Journal of Cleaner Production 2015, 96, 501–519.
67. Maes WH; Verbist B, Increasing the sustainability of household cooking in developing countries: Policy implications. Renewable and Sustainable Energy Reviews 2012, 16, (6), 4204–4221.
68. Feng L; Smith SJ; Braun C; Crippa M; Gidden MJ; Hoesly R; Klimont Z; van Marle M; van den Berg M; van der Werf GR, The generation of gridded emissions data for CMIP6. Geosci. Model Dev 2020, 13, (2), 461–482.
69. Hoesly RM; Smith SJ; Feng L; Klimont Z; Janssens-Maenhout G; Pitkanen T; Seibert JJ; Vu L; Andres RJ; Bolt RM; Bond TC; Dawidowski L; Kholod N; Kurokawa JI; Li M; Liu L; Lu Z; Moura MCP; O'Rourke PR; Zhang Q, Historical (1750–2014) anthropogenic emissions of reactive gases and aerosols from the Community Emissions Data System (CEDS). Geosci. Model Dev 2018, 11, (1), 369–408.
70. O'Rourke PR; Smith SJ; Mott A; Ahsan H; McDuffie EE; Crippa M; Klimont Z; McDonald B; Wang S; Nicholson MB; Feng L; Hoesly RM, CEDS v_2021_02_05 Release Emission Data. In Community Emissions Data System, Ed. 10.5281/zenodo.4074245, 2021.
71. Zhang Y; Liu J; Tao W; Xiang S; Liu H; Yi K; Yang H; Xu J; Wang Y; Ma J; Wang X; Hu J; Wan Y; Wang X; Tao S, Impacts of chlorine emissions on secondary pollutants in China. Atmospheric Environment 2021, 246, 118177.
72. Liu L; Liu Y; Wen W; Liang L; Ma X; Jiao J; Guo K, Source Identification of Trace Elements in PM2.5 at a Rural Site in the North China Plain. Atmosphere 2020, 11, (2), 179.
73. McNamara SM; Kolesar KR; Wang S; Kirpes RM; May NW; Gunsch MJ; Cook RD; Fuentes JD; Hornbrook RS; Apel EC; China S; Laskin A; Pratt KA, Observation of Road Salt Aerosol Driving Inland Wintertime Atmospheric Chlorine Chemistry. ACS Central Science 2020, 6, (5), 684–694. [PubMed: 32490185]
74. Kolesar KR; Mattson CN; Peterson PK; May NW; Prendergast RK; Pratt KA, Increases in wintertime PM2.5 sodium and chloride linked to snowfall and road salt application. Atmospheric Environment 2018, 177, 195–202.
75. Haskins JD; Jaeglé L; Shah V; Lee BH; Lopez-Hilfiker FD; Campuzano-Jost P; Schroder JC; Day DA; Guo H; Sullivan AP; Weber R; Dibb J; Campos T; Jimenez JL; Brown SS; Thornton JA, Wintertime Gas-Particle Partitioning and Speciation of Inorganic Chlorine in the

Lower Troposphere Over the Northeast United States and Coastal Ocean. Journal of Geophysical Research: Atmospheres 2018, 123, (22), 12,897–12,916.

76. Jaiprakash; Singhai A; Habib G; Raman RS; Gupta T, Chemical characterization of PM1.0 aerosol in Delhi and source apportionment using positive matrix factorization. Environmental Science and Pollution Research 2017, 24, (1), 445–462. [PubMed: 27726085]
77. Chang S; McDonald-Buller E; Kimura Y; Yarwood G; Neece J; Russell M; Tanaka P; Allen D, Sensitivity of urban ozone formation to chlorine emission estimates. Atmospheric Environment 2002, 36, (32), 4991–5003.
78. Sarwar G; Bhave PV, Modeling the Effect of Chlorine Emissions on Ozone Levels over the Eastern United States. Journal of Applied Meteorology and Climatology 2007, 46, (7), 1009–1019.
79. Li L; Yin S; Huang L; Yi X; Wang Y; Zhang K; Ooi CG; Allen DT, An emission inventory for Cl2 and HOCl in Shanghai, 2017. Atmospheric Environment 2020, 223, 117220.
80. Yi X; Yin S; Huang L; Li H; Wang Y; Wang Q; Chan A; Traoré D; Ooi MCG; Chen Y; Allen DT; Li L, Anthropogenic emissions of atomic chlorine precursors in the Yangtze River Delta region, China. Science of The Total Environment 2021, 771, 144644. [PubMed: 33736175]

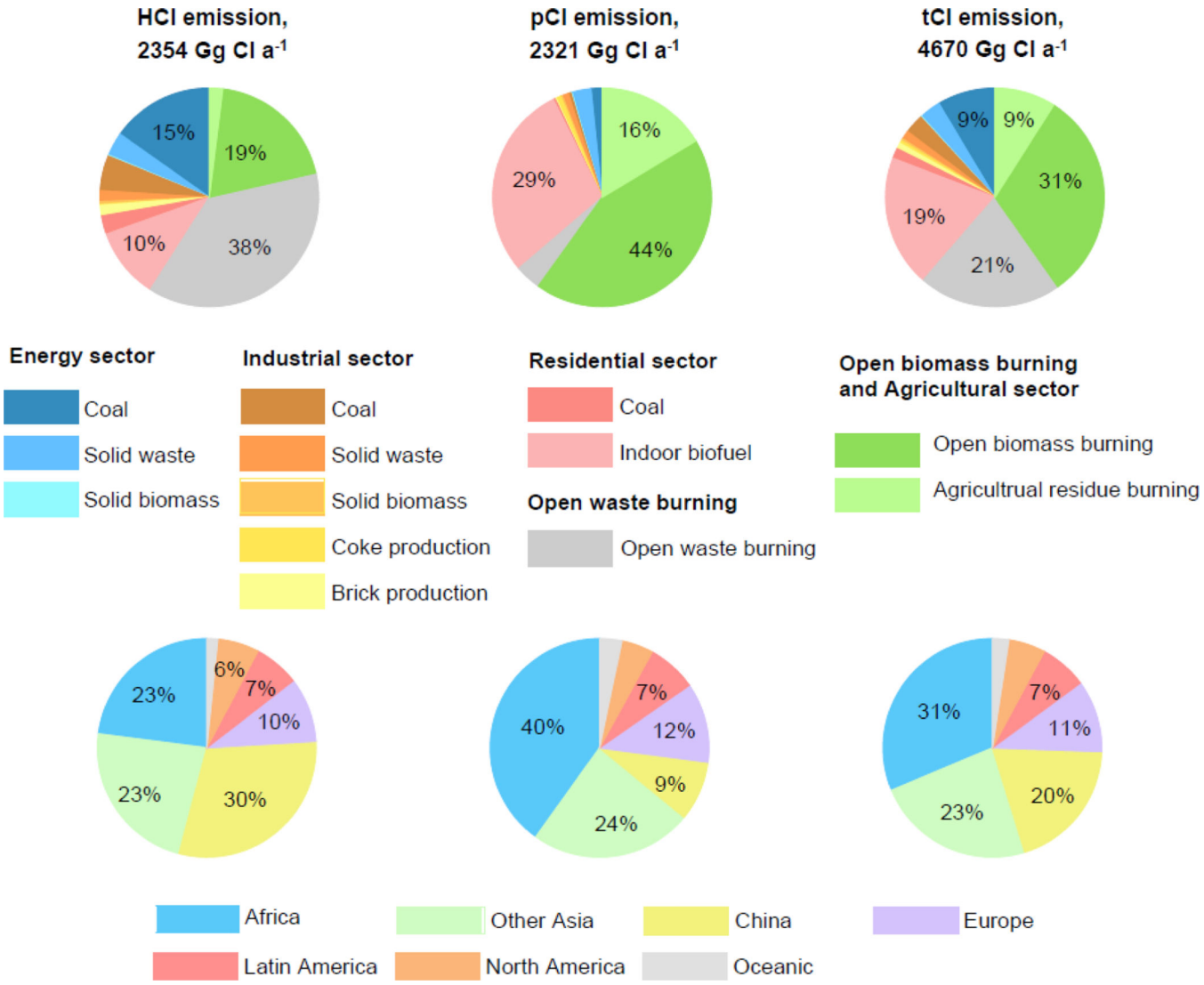

Figure 1.

Pie charts show fractions of HCl, pCl and tCl (HCl + pCl) annual emissions in 2014 by source sectors (a, b, c) and by emission regions (d, e, f). Percentage of emission by each major contributor (i.e., contribute more than 5%) is marked on the pie chart. Total emissions of HCl, pCl, and tCl are also marked.

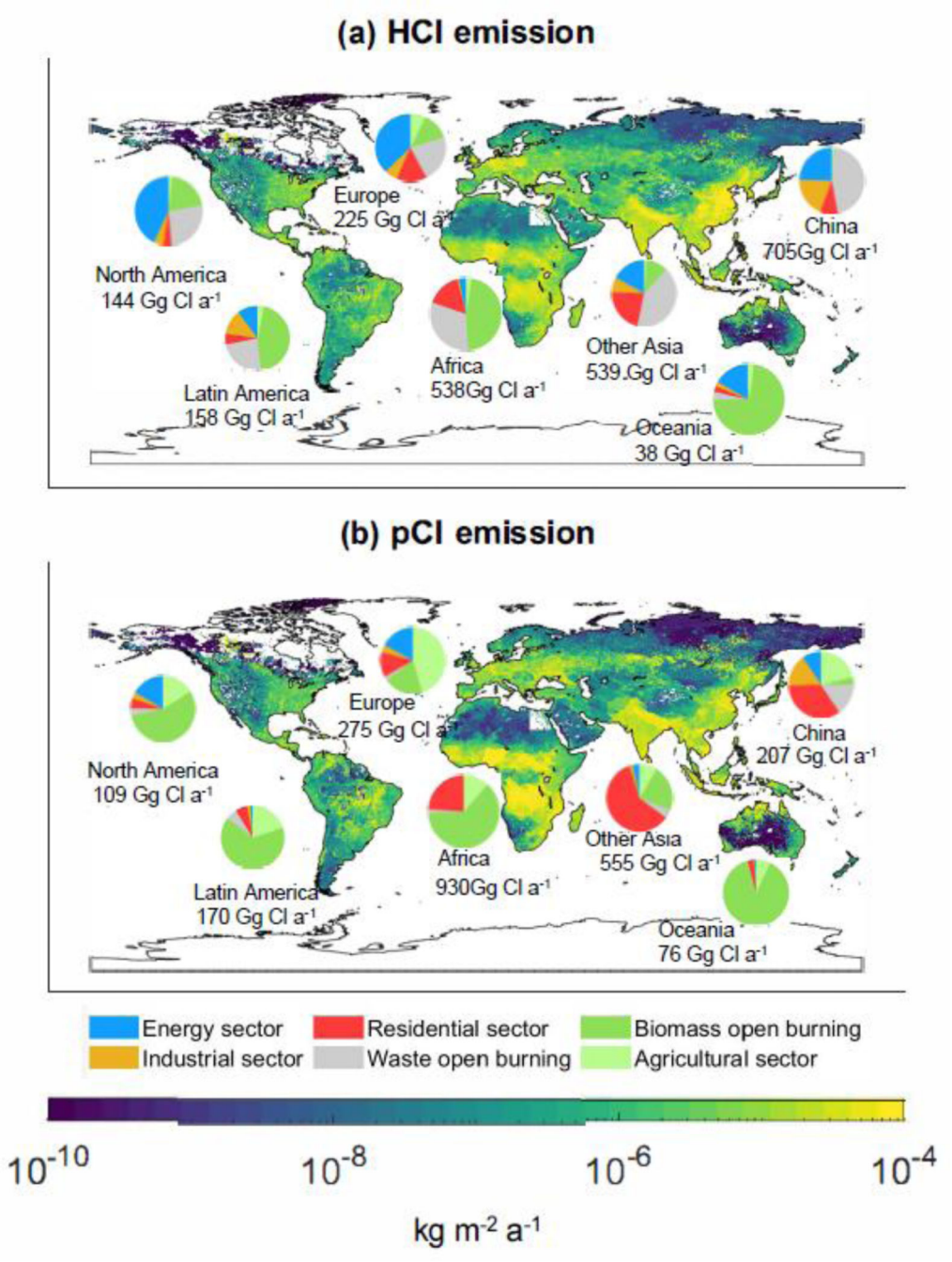

Figure 2.

Geographical distributions of (a) HCl and (b) pCl emission fluxes in 2014. The embedded pie charts and texts show the annual emissions from difference source sectors for 7 regions.

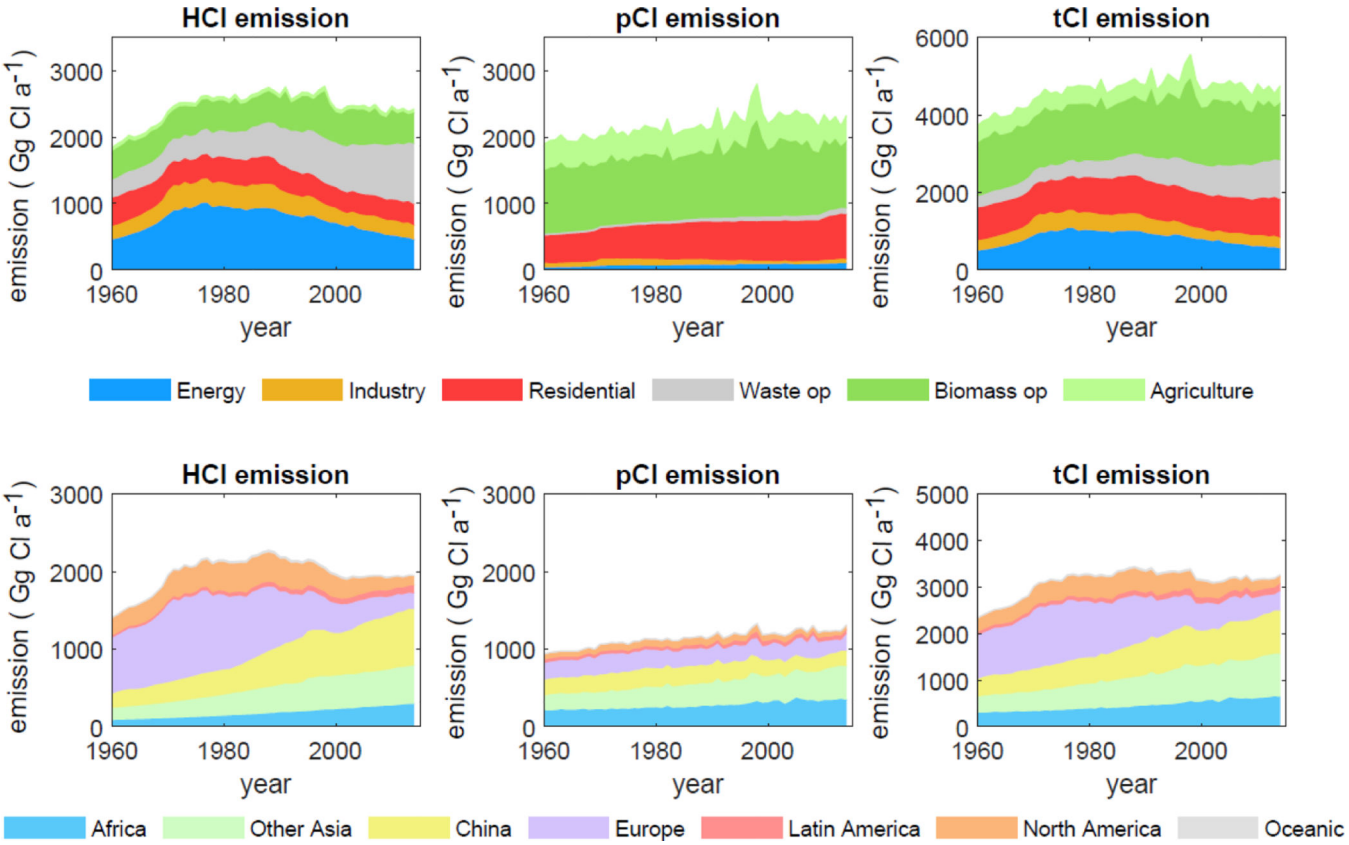

Figure 3.

Temporal trends of annual HCl, pCl and tCl emissions by sectors (upper panels) and regions (lower panels). Emissions from open biomass burning are excluded in the lower panels.

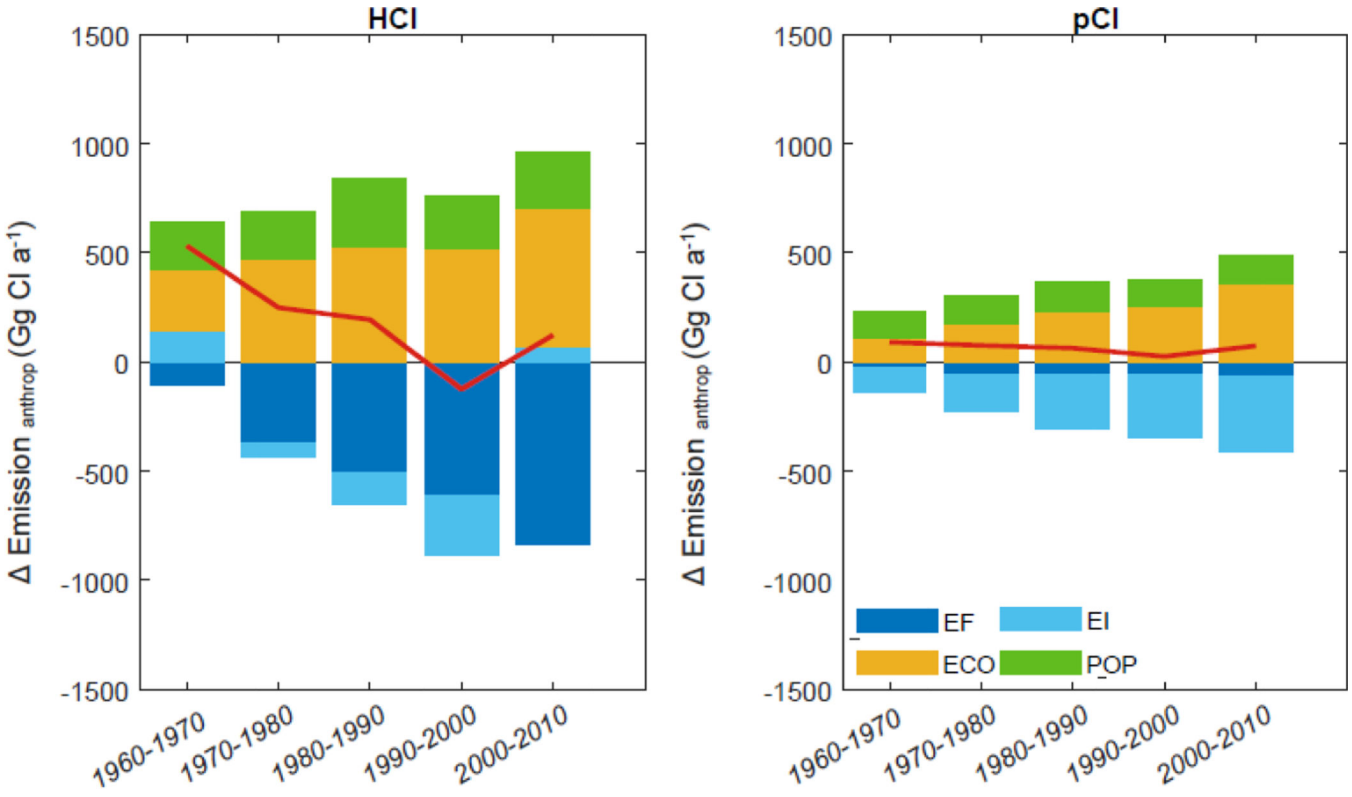

Figure 4.

Decomposition of the changes in global HCl and pCl emissions within each decade using method described in Section 2.4 and Text S3. Open biomass burning is excluded in the analysis. The sum of contributions of all four factors (i.e., EF, EI, ECO, POP) are represented by red lines.

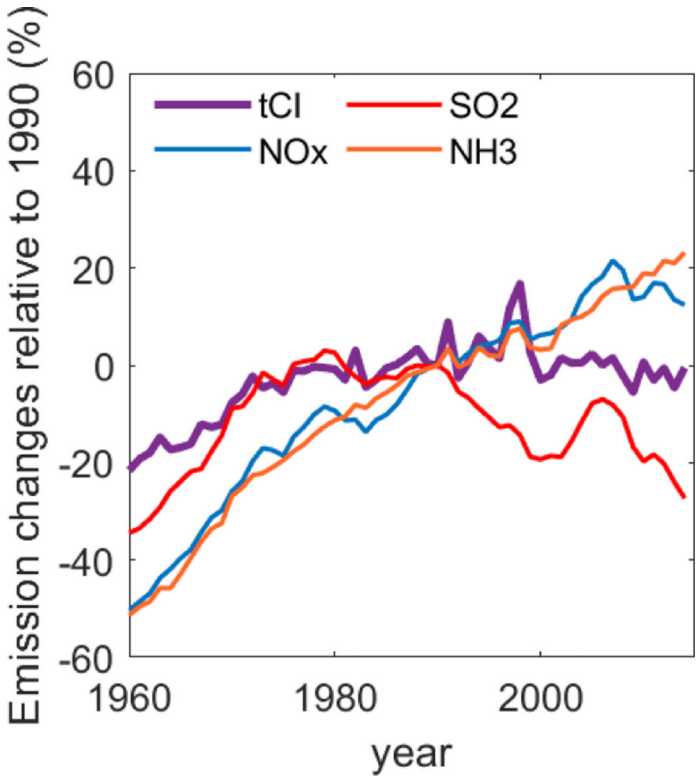

Figure 5.

Temporal trends of tCl (HCl+pCl), NO_x, SO_2 and NH_3 emissions between 1960–2014. Data are shown for the percentage changes relative to a baseline year of 1990.

Table 1

List of sectors and fuel types and emission factors collected from literature and dataset.

Sector	Subsector	Fuel	Emission factor (g/kg)[a]			
			HCl	Refs.	pCl	Refs.
Energy production	Coal combustion	Anthracite	Calculated based on chlorine content and removal efficiency (Text S2.1)			
		Coke				
		Bituminous coal				
		Lignite				
		Peat				
	Waste combustion	Municipal waste[b]	3.20	44	1.74[c]	44, 45
		Industrial waste[b]	3.20	44	1.74[c]	44, 45
	Biomass combustion	Solid biomass[b]	0.06	46, 47	0.05[c]	46, 47
Industrial processes	Coal combustion	Anthracite	Calculated based on chlorine content and removal efficiency (Text S2.1)			
		Coke				
		Bituminous coal excluding coke and brick production				
		Lignite				
		Peat				
	Brick production		Calculated based on chlorine content (Text S2.2)			
	Coke production		Calculated based on uncontrolled EF for PM, HCl and pCl weight percentage, chlorine content in different countries and removal efficiency (Text S2.2)			
	Waste combustion	Municipal waste[b]	3.20	44	1.74[c]	44, 45
		Industrial waste[b]	3.20	44	1.74[c]	44, 45
	Biomass combustion	Solid biomass[b]	0.06	46, 47	0.05[c]	46, 47
Residential household	Coal combustion	Anthracite	Calculated based on chlorine content (Text S2.1)			
		Coke				
		Bituminous Coal				
		Lignite				
		Peat				
	Indoor biofuel combustion	Charcoal	0.06	46, 47	0.05[c]	46, 47
		Firewood	0.06	46, 47	0.05[c]	46, 47
		Brushwood	0.06	46, 47	0.05[c]	46, 47
		Straw	0.18	46, 47	0.57	46, 47
		Dung	0.038	46, 47	0.35	46, 47
		Corn cob	0.18	46, 47	0.57	46, 47

Sector	Subsector	Fuel	Emission factor (g/kg)[a]			
			HCl	Refs.	pCl	Refs.
Open waste burning			Calculate based on country-level waste composition and chlorine content in different types of waste (Text S2.3)			
Open biomass burning	Biomass burning	Savannah and grassland	0.13	46, 47	0.30[c]	46, 47
		Temperate forest	0.04	46, 47	0.27[c]	46, 47
		Boreal forest	0.13	46, 47	0.22[c]	46, 47
		Deforestation	0.13	46, 47	0.17[c]	46, 47
		Peat	0.01	46, 47	0.11[c]	46, 47
Agricultural processes	Biomass burning	Agricultural residue	0.18	46, 47	0.30[b]	46, 47

[a], the mean value was used when multiple records were available. Industrial waste is assumed to have the same EF as municipal waste because of the lack of waste composition information; Solid biomass used in energy and industry sector and charcoal used in residential are assumed to have same EF as wood used in residential sector due to similar chlorine content since they are made from biomass;

[b], uncontrolled EF, controlled EF are calculated based on uncontrolled values time removal efficiency described in Text S2.1;

[c], calculated by EF of PM and mass percentage of Cl in total PM.

Table 2

Emissions in different sectors in 2014. The values in parenthesis show the estimated uncertainty represented by the interquartile range (i.e., 25th to 75th percentiles).

Sector	Subsector	Emission (Gg Cl a^{-1})					
		1960		1990		2014	
		HCl	pCl	HCl	pCl	HCl	pCl
Energy	Coal combustion	448 (289 – 530)	40 (26 – 46)	775 (512 – 907)	53 (35 – 61)	358 (225 – 419)	38 (25 – 44)
	Solid waste combustion	0.3 (0.2 – 0.4)	0.1 (0 – 0.2)	79 (50 – 107)	28 (16 – 36)	82 (53 – 110)	66 (43 – 89)
	Solid Biomass combustion	0.3 (0.2 – 0.3)	0.2 (0 – 0.6)	2 (1 – 3)	1 (0 – 3)	4 (3 – 5)	3 (2 – 8)
Industry	Coal combustion	178 (107 – 211)	16 (9 – 18)	199 (124 – 236)	10 (6 – 11)	122 (61 – 153)	10 (5 – 11)
	Solid waste combustion	2 (1 – 3)	1 (1 – 2)	69 (43 – 93)	28 (17 – 37)	38 (23 – 51)	22 (14 – 29)
	Solid Biomass combustion	3 (3 – 4)	3 (2 – 7)	16 (13 – 18)	8 (4 – 21)	9 (7 – 11)	6 (3 – 17)
	Coke production	11 (6 – 22)	50 (21 – 70)	94 (6 – 110)	27 (15 −39)	4 (3 – 8)	16 (3 – 17)
	Brick production	2 (0 – 3)	0.2 (0 – 2)	29 (16– 37)	3 (1 – 5)	37 (27 – 51)	4 (2 – 7)
Residence	Coal combustion	277 (174 – 339)	28 (18 – 34)	155 (105 – 184)	16 (11 – 19)	65 (39 – 79)	7 (4 – 8)
	Indoor biofuel burning	141 (88 – 189)	386 (154 – 564)	214 (154 – 298)	558 (240 – 844)	247 (175 – 351)	669 (275 – 981)
Open waste burning		257 (221 – 361)	49 (34 – 84)	534 (478 – 758)	54 (48 – 76)	886 (792 – 1263)	89 (79– 126)
Open biomass burning		418 (180 – 569)	954 (335 – 1233)	428 (186 – 560)	969 (344 – 1238)	457 (246 – 643)	1010 (428 – 1379)
Agricultural residue burning		48 (7 – 56)	387 (44 – 525)	47 (6 – 54)	385 (44 – 522)	47 (7 – 57)	379 (45 – 543)
Total		**1786 (1076 – 2288)**	**1915 (644 – 2586)**	**2641 (1694 – 3375)**	**2140 (781 – 2912)**	**2354 (1661 – 3200)**	**2321 (930 – 3264)**